Comparative Assessment of Boiling Heat Transfer Predictability of System Codes MARS-KS and TRACE in Helically Coiled Tubes

Seongman Jeong, Yunseok Lee, Taewan Kim*
Department of Safety Engineering, Incheon National University, 119 Academy-ro, Yeonsu-gu, Incheon 22012, Republic of Korea
**Corresponding author: taewan.kim@inu.ac.kr*

Keywords : MARS-KS, TRACE, heat transfer coefficient, helically coiled tube

1. Introduction

Recently, Small modular reactors (SMRs) have been actively developed to meet the increasing energy demand and to achieve decarbonization. Most SMRs employ helical coil steam generators (HCSGs) owing to their compactness and high thermal efficiency. The curved geometry of the HCSG induces secondary flows that enhance heat transfer while increasing pressure drop, making its thermal-hydraulic behavior distinct from that of straight-tube heat exchangers. Therefore, it is essential to incorporate these characteristics when analyzing HCSG using system codes.

MARS-KS, a regulatory confirmatory code of the Republic of Korea, incorporates only the heat transfer model for helical tubes [1], whereas TRACE, developed by the U.S. Nuclear Regulatory Commission (NRC), includes both heat transfer and pressure drop models [2]. However, the prediction capability of both codes for heat transfer in helical tubes has not yet been fully assessed. Accordingly, this study evaluated the heat transfer prediction capability of MARS-KS 2.0 and TRACE V5 Patch 8 against the experiments by Santini et al. [3], Chang et al. [4], and Xiao et al. [5-7].

2. Heat Transfer Models in System codes

In this section, the helical-tube heat transfer correlations employed in MARS-KS and TRACE are described.

2.1 MARS-KS

For single-phase turbulent heat transfer in helical tubes, MARS-KS applies the Mori-Nakayama [8] correlation, which is expressed as:

$$Nu = \begin{cases} \frac{1}{41.0} Re^{0.8333} Pr^{0.4} \left(\frac{d}{D_c}\right)^{\frac{1}{12}} \left[1 + \frac{0.061}{\left[Re\left(\frac{d}{D_c}\right)^{2.5}\right]^{\frac{1}{6}}}\right] & (Pr > 1) \\ \frac{Pr}{26.2\left(Pr^{\frac{2}{3}} - 0.074\right)} Re^{0.8} \left(\frac{d}{D_c}\right)^{\frac{1}{10}} \left[1 + \frac{0.098}{\left[Re\left(\frac{d}{D_c}\right)^{2}\right]^{\frac{1}{5}}}\right] & (Pr < 1) \end{cases} \quad (1)$$

where Nu denotes the Nusselt number, Re is the Reynolds number, and Pr is the Prandtl number, while d and D_c represent the tube diameter and coil diameter, respectively. The Mori–Nakayama correlation is categorized based on the Prandtl number [8]; however, MARS-KS currently implements only the form applicable to $Pr < 1$ conditions [1].

For the nucleate boiling regime, the Chen [9] correlation is employed. The Chen correlation calculates the boiling heat transfer coefficient by the superposition of the forced convection and pool boiling components as follows [9]:

$$q''_{NB} = h_{FC}(T_w - T_f)F + h_{PB}(T_w - T_{sat})S \quad (2)$$

where q''_{NB} denotes the nucleate boiling heat flux, T_w is the wall temperature, T_f is the fluid temperature, and T_{sat} is the saturation temperature. h_{FC} and h_{PB} represent the forced convection and pool boiling heat transfer coefficients, respectively. The Reynolds number factor, F and suppression factor, S are defined as follows:

$$F = \begin{cases} 1.0 & (X_{tt}^{-1} < 0.1) \\ 2.34(X_{tt}^{-1} + 0.213)^{0.736} & (X_{tt}^{-1} > 0.1) \end{cases} \quad (3)$$

$$S = \begin{cases} [1 + 0.12(Re_{TP})^{1.14}]^{-1} & (Re_{TP} < 32.5) \\ [1 + 0.42(Re_{TP})^{0.78}]^{-1} & (32.5 \le Re_{TP} < 70.0) \\ 0.0797 & (Re_{TP} \ge 32.5) \end{cases} \quad (4)$$

$$X_{tt} = \left[\left(\frac{1-x}{x}\right)^{0.9} \left(\frac{\rho_g}{\rho_f}\right)^{0.5} \left(\frac{\mu_f}{\mu_g}\right)^{0.1}\right] \quad (5)$$

$$Re_{tp} = Min(70, 10^{-4} Re \cdot F^{1.25}) \quad (6)$$

where X_{tt} is the Martinelli parameter and Re_{tp} is the two-phase Reynolds number, which are defined in Eqs. (5) and (6), respectively. The forced convection term, h_{FC}, is evaluated using the Mori–Nakayama correlation of Eq. (1), whereas the pool boiling term, h_{PB}, is calculated by the Forster–Zuber [10] correlation as follows [1]:

$$h_{PB} = 0.00122\left(\frac{k_f^{0.79} c_{pf}^{0.45} \rho_f^{0.49}}{\sigma^{0.5} \mu_f^{0.29} h_{fg}^{0.24} \rho_g^{0.24}}\right)(T_w - T_{sat})^{0.24}(P_w - P)^{0.75} \quad (7)$$

where the subscripts f and g denote the liquid and vapor phases, respectively, and h_{fg} is the latent heat of vaporization. Also, in MARS-KS, an upper limit of 50,000 W/m²·K is applied on the heat transfer coefficient of each term in the Chen correlation.

2.2 TRACE

For single-phase convective heat transfer in helical tubes, TRACE adopts the Ebadian and Dong correlation [11]. For laminar flow, the correlation is given as:

$$\frac{Nu_c}{Nu_s} = \left[\left(4.364 + \frac{4.636}{x_3}\right)^3 + 1.816 \cdot \left(\frac{De}{x_4}\right)^{\frac{3}{2}}\right]^{\frac{1}{3}} \quad (8)$$

$$x_3 = \left(1 + \frac{1342}{De^2 \cdot Pr}\right)^2 \; and \; x_4 = 1 + \frac{1.15}{Pr} \quad (9)$$

where Nu_c and Nu_s represent the Nusselt numbers for the curved and straight pipes, respectively, and De is the Dean number. The denominator terms x_3 and x_4 are defined in Eq. (9)

For turbulent flow, the correlation is expressed as:

$$\frac{Nu_c}{Nu_s} = \begin{cases} 1 + 3.6 \cdot \left[1 - \frac{d}{D_c}\right] \cdot \left(\frac{d}{D_c}\right)^{0.8} & (10) \\ 1 + 3.4 \cdot \frac{d}{D_c} & (11) \end{cases}$$

Eq. (10) is applied for the conditions of 20,000 < Re < 150,000 and 5 < $\frac{D_c}{d}$ < 84, whereas Eq. (11) is employed for 1,500 < Re < 20,000. For boiling conditions, TRACE models the total heat flux as a superposition of forced convection, pool boiling, and initiation of nucleate boiling contributions [2]:

$$q''_{NB} = (q''_{FC} + (q''_{PB} - q''_{BI})) \quad (12)$$

where q''_{FC}, q''_{PB}, and q''_{BI} represent the forced convection, pool boiling, and boiling initiation heat fluxes, respectively. The forced convection contribution is evaluated using the Ebadian and Dong correlation, while the pool boiling term is obtained from the Gorenflo correlation [12]:

$$h_{PB} = \left(h_0 \cdot F_p / q''^n_0\right)^{\frac{1}{1-n}} \cdot (T_w - T_{Sat})^{\frac{n}{1-n}} \quad (13)$$

$$F_p = 1.73 \cdot \left(\frac{P}{P_{Crit}}\right)^{0.27} + \left(6.1 + \frac{0.68}{1 - \frac{P}{P_{Crit}}}\right) \cdot \left(\frac{P}{P_{Crit}}\right)^2 \quad (14)$$

$$n = 0.9 - 0.3 \cdot \left(\frac{P}{P_{Crit}}\right)^{0.15} \quad (15)$$

where P_{crit} denotes the critical pressure, and h_0 and q''_0 are the reference values of 5,600 W/m²·K and 20,000 W/m², respectively. In addition, the pressure effect term F_p and the exponent n are defined in Eq. (14) and (15), respectively.

3. Experimental Database and Input Model

3.1 Experimental database

For the assessment, the boiling heat transfer experiments conducted by Santini et al. [3], Chang et al. [4], and Xiao et al. [5] were employed as benchmark data. Furthermore, the dryout experiments by Xiao et al. [6, 7] were included to evaluate the code prediction capability in the high-quality region. The experiments cover a wide range of pressure from 2 to 8 MPa with various heat flux and mass flux conditions, and the detailed test conditions are given in Tables I and II.

Table I: Experimental geometric information

Authors	d_i [mm]	D_c [mm]	Tube length [m]
Santini et al. [3]	12.49	1000	32.0
Chang et al. [4]	8.0	650	2.45 (height)
Xiao et al. [5]	14.5	180	8.00
Xiao et al. [6, 7]	12.5 14.5	180 280 380	8.00

Table II: Experimental Test Conditions

Authors	Pressure [MPa]	Mass flux [kg/m²·s]	Heat flux [kW/m²]
Santini et al. [3]	2.0-6.0	200-820	46-200
Chang et al. [4]	8.0	500-1000	100-200
Xiao et al. [5]	2.0-7.6	400-1000	100-500
Xiao et al. [6, 7]	2.0-7.6	400-800	200-400

3.2 Assessment model description

Since helical-tube geometry cannot be directly represented in system codes, an equivalent inclined pipe model was adopted to simulate the helical tubes. The nodalization for each experiment was established on the basis of a node sensitivity analysis performed with MARS-KS, and the resulting input model specifications are provided in Table III. The identical nodalization was then applied to TRACE to enable a consistent quantitative comparison between the two codes. Fig. 1 illustrates the input model configuration employed for both system codes.

Table III: Nodalization for modeling

Authors	Inclined angle [°]	Number of nodes	Node length range [m]
Santini et al. [3]	14.115	60	0.2-0.8
Chang et al. [4]	5.065	27	0.255-2.775
Xiao et al. [5]	5.996	36	0.1-0.45
Xiao et al. [6]	5.996	25-47	0.05-0.4
Xiao et al. [7]	5.996	29	0.2-0.4

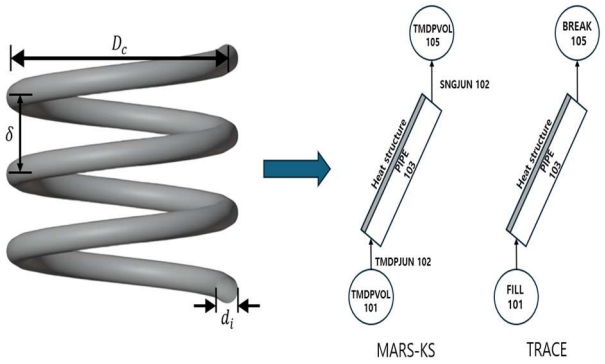

Fig. 1. Helical-tube input models configuration

4. Assessment Results

The prediction capability of both system codes was evaluated using the selected experimental data. The assessment results of MARS-KS indicated that the code generally overpredicted the heat transfer coefficients relative to the experimental data, as depicted in Fig. 2. In addition, the calculated results exhibited a tendency to converge to approximately 50,000 W/m²·K, the aforementioned upper bound. However, as confirmed in Fig. 4, the overprediction tendency persisted even when this upper bound was removed. TRACE exhibited a similar overprediction tendency; however, the degree of overprediction was considerably larger than that observed in MARS-KS.

The quantitative comparison based on the root-mean-square errors (RMSEs) is summarized in Table IV. The results confirm that TRACE exhibited lower prediction accuracy compared to MARS-KS. In addition, the overall assessment results clearly indicate that the current heat transfer model employed in TRACE needs to be further improved.

When the dryout experiments by Xiao et al. [6, 7] were incorporated into the assessment, both codes yielded highly scattered predictions with significant deviations from the experimental data, as depicted in Fig. 3. In MARS-KS, the dryout occurrence in helical tubes was determined solely on the basis of the void fraction, where the onset of first and total dryout was assumed at void fractions exceeding 0.99 and 0.999, respectively [1]. This simplified criterion did not account for the physical mechanisms governing dryout in helical tubes and therefore failed to reproduce the experimental observations. On the other hand, although TRACE implements the mechanistic dryout model proposed by Berthoud and Jayanti [13], the code was also unable to reproduce the dryout behavior observed in the experiments [2]. These findings indicated that further improvement of the dryout models is required in both codes to adequately predict the dryout phenomena in helical tubes.

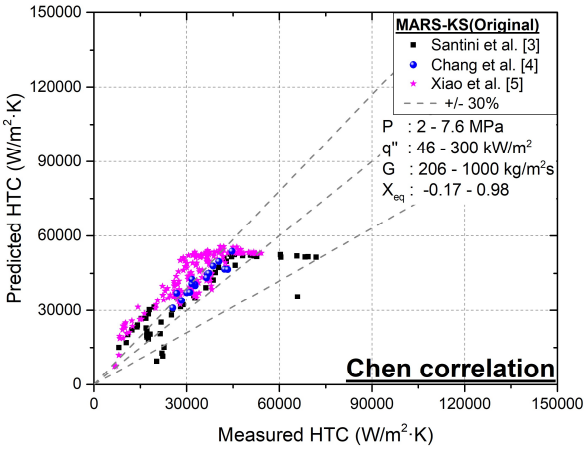

(a) MARS-KS(Original)

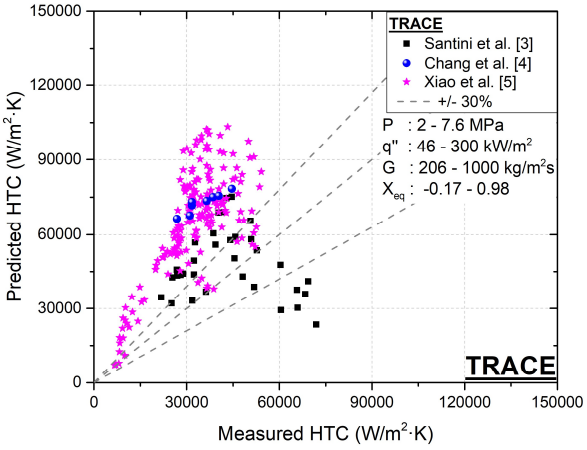

(b) TRACE

Fig. 2. Assessment results (without dryout experiments)

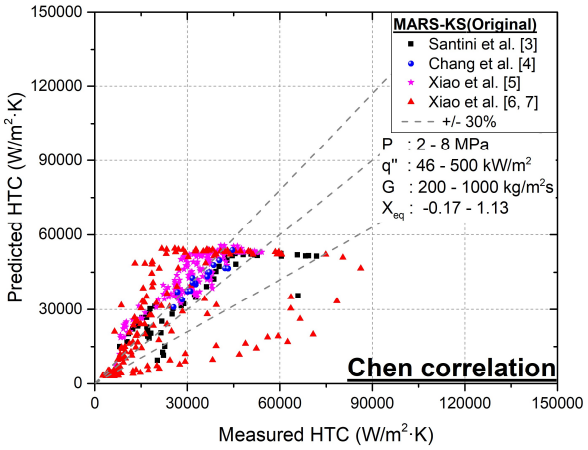

(a) MARS-KS(Original)

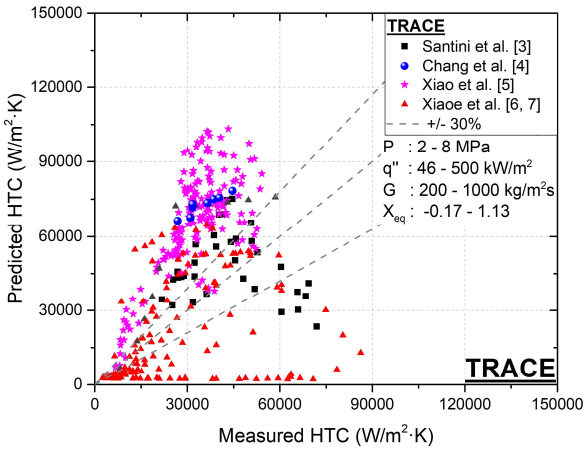

(b) TRACE

Fig. 3. Assessment results (with dryout experiments)

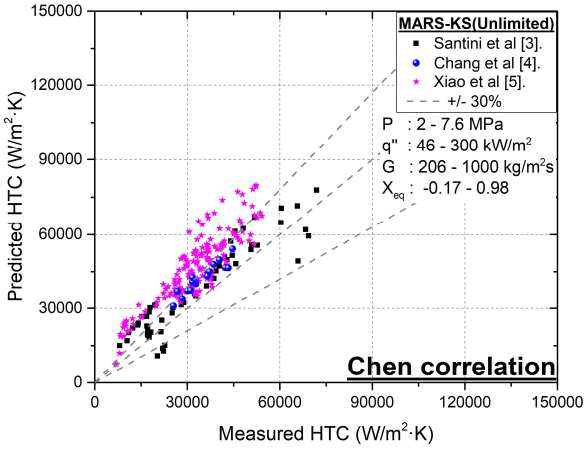

Fig. 4. MARS-KS (Unlimited) Assessment results

Table IV: Experimental Assessment Results

EXP	Root-Mean-Square-Error (RMSE)	
	MARS-KS	TRACE
Santini et al. [3]	0.2337	0.4826
Chang et al. [4]	0.3753	1.1231
Xiao et al. [5]	0.4144	1.1658
Xiao et al. [6, 7]	0.6819	0.7439
Total	0.5380	0.9565

5. Conclusions

In this study, a comparative assessment of the system codes, MARS-KS and TRACE, was performed with respect to the heat transfer predictions in helical tubes. The boiling heat transfer experiments by Santini et al., Chang et al., and Xiao et al. were employed as benchmark data.

The results indicated that both codes overpredicted the heat transfer coefficients in helical tubes. In particular, TRACE showed a considerably larger deviation from the experimental data than MARS-KS. The assessment results also clearly indicated that the helical-tube heat transfer model currently implemented in TRACE should be further improved.

On the other hand, when the dryout experiments were incorporated into the assessment, neither code adequately reproduced the experimental observations. In MARS-KS, the simplified void fraction-based criterion failed to adequately predict the experimental dryout behavior. Likewise, even though TRACE employed the mechanistic dryout model proposed by Berthoud and Jayanti, it also failed to reproduce the dryout behavior in the experiments. These results clearly confirmed that further improvement is essential for both codes in order to improve the dryout predictions. As future work, enhancements to both the heat transfer and dryout models will be performed, along with further comparison against an extended range of experimental data.

ACKNOWLEDGMENT

This work was supported by the Nuclear Safety Research Program through the Regulatory Research Management Agency for SMRSs (RMAS) and the Nuclear Safety and Security Commission (NSSC) of Republic of Korea (No. 1500-1501-409).

REFERENCES

[1] Korea Atomic Energy Research Institute (KAERI), "MARS-KS CODE MANUAL, Volume V: Models and Correlations", KAERI/TR-3872/2009, 2009.

[2] U.S. Nuclear Regulatory Commission (NRC), “TRACE V5.0 PATCH 8 USER’S MANUAL, Volume I: Input Specification”, Division of Safety Analysis, Office of Nuclear Regulatory Research, U.S. NRC, Washington, DC 2023.
[3] L. Santini, A. Cioncolini, M. T. Butel, and M. E. Ricotti, Flow boiling heat transfer in a helically coiled steam generator for nuclear power applications, International Journal of Heat and Mass Transfer, Vol. 92, p. 91-99, 2016.
[4] F. Chang, Y. Liu, J. Lou, Y. Shang, H. Hu, and H. Li, Experimental investigation on flow boiling heat transfer characteristics of water and circumferential wall temperature inhomogeneity in a helically coiled tube, Chemical Engineering Science, Vol. 272, 118592, 2023.
[5] Y. Xiao, Z. Hu, S. Chen and H. Gu, Experimental investigation of boiling heat transfer in helically coiled tubes at high pressure, Annals of Nuclear Energy, Vol.113, p. 409-419 2018.
[6] Y. Xiao, Z. Hu, S. Chen and H. Gu, Experimental investigation and prediction of post-dryout heat transfer for steam-water flow in helical coils, International Journal of Heat and Mass Transfer, Vol.127, p. 515-525, 2018.
[7] Y. Xiao, Z. Hu, S. Chen, and H. Gu, Experimental study on dryout characteristics of steam-water flow in vertical helical coils with small coil diameters, Nuclear Engineering and Design, Vol.335, p. 303-313, 2018.
[8] Y. Mori, W. Nakayama, Study on Forced Convective Heat Transfer in Curved Pipes, Int. J. Mass Transfer, Vol. 10, pp.37-59, 1967.
[9] J. C. Chen, A Correlation for Boiling Heat Transfer to Saturated Fluids in Convective Flow, Am. Soc. Mech. 63-HT-34, 1963.
[10] H. K. Forster, and N. Zuber, Dynamics of Vapor Bubbles and Boiling Heat Transfer, AIChE Journal, Vol. 1, No. 4, pp. 531-535, 1955.
[11] M.A. Ebadian, and Z.F. Dong, "Forced Convection, Internal Flow in Ducts, Chapter 5 of the Handbook of Heat Transfer, edited by W.M. Rohsenow, J.P. Hartnett and Y.I. Cho” McGraw Hill, 1998.
[12] D. Gorenflo, "Pool Boiling, Chapter Ha of VDI-Heat Atlas,” VDI-Verlag, Dusseldorf, 1993.
[13] G. Berthoud, and S. Jayanti, Characterization of dryout in helical coils, International Journal of Heat and Mass Transfer, Vol. 33(7), pp. 1451-1463, 1990.